available at www.sciencedirect.com

ScienceDirect

journal homepage: www.ejconline.com

Role of homologous recombination in trabectedin-induced DNA damage

M. Tavecchio[a], M. Simone[a], E. Erba[a], I. Chiolo[b,c,d], G. Liberi[b,c], M. Foiani[b,c], M. D'Incalci[a], G. Damia[a,*]

[a]Department of Oncology, Istituto di Ricerche Farmacologiche "Mario Negri", Via La Masa 19, 20156 Milan, Italy
[b]FIRC Institute of Molecular Oncology Foundation, Via Adamello 16, 20139, Milan, Italy
[c]Dipartimento di Scienze Biomolecolari e Biotecnologie, Università degli Studi di Milano, Via Celoria 26, 20133, Milan, Italy
[d]On leave to: Department of Genome and Computational Biology, Lawrence Berkeley National Laboratory, Berkeley, CA 94720, USA

ARTICLE INFO

Article history:
Received 28 December 2007
Accepted 4 January 2008
Available online 19 February 2008

Keywords:
Trabectedin
DNA repair
HR and NER

ABSTRACT

Trabectedin (ET-743, Yondelis) is a natural marine compound with antitumour activity currently undergoing phase II/III clinical trials. The mechanism of the drug's action is still to be defined, even though it has been clearly demonstrated the key role of Nucleotide Excision Repair (NER). To get further insights into the drug's mode of action, we studied the involvement of the DNA-double strand break repair (DNA-DSB) pathways: homologous and non-homologous recombination, both in budding yeasts and in mammalian cells and the possible cross-talk between NER and these repair pathways. Budding yeasts and mammalian cells deficient in the non-homologous end-joining pathway were moderately sensitive to trabectedin, while systems deficient in the homologous recombination pathway were extremely sensitive to the drug, with a 100-fold decrease in the IC50, suggesting that trabectedin-induced lesions are repaired by this pathway. The induction of Rad51 foci and the appearance of γ-H2AX were chosen as putative markers for DNA-DSBs and were studied at different time points after trabectedin treatment in NER proficient and deficient systems. Both were clearly detected only in the presence of an active NER, suggesting that the DSBs are not directly caused by the drug, but are formed during the processing/repair of the drug- induced lesions.

1. Introduction

Trabectedin (ecteinascidin-743, ET-743, Yondelis) is a tetrahydroisoquinoline alkaloid isolated from the Carribean tunicate *Ecteinaiscidia turbinata* in the late 1960s. This compound has shown very interesting preclinical and clinical activity on several malignancies, including ovarian carcinoma and sarcomas.[1–7]

Trabectedin consists of three fused tetrahydroisoquinoline rings referred to as subunits A, B and C. Even if there is not yet direct evidence that DNA is trabectedin's primary target, the available experimental data strongly suggest that its cytotoxic effects depend on the interaction with DNA. Trabectedin has been shown to bind to the N2 position of guanine in the minor groove of DNA with some sequence specificity.[8] Subunits A and B of the drug are responsible for DNA recognition and binding, whereas subunit C protrudes out of the minor groove perpendicular to the helix axis.[9] It was suggested that the C ring interaction with nuclear proteins could account for the cytotoxic effects of trabectedin, but recently it has been

* *Corresponding author:* Tel.: +39 0239014473; fax: +39 023546277.
E-mail address: damia@marionegri.it (G. Damia).
0959-8049/$ - see front matter
doi:10.1016/j.ejca.2008.01.003

published that PM00128, a trabectedin analogue lacking the C subunit, has shown a biological activity superimposable to that of trabectedin.[10]

We and others have previously demonstrated a unique pattern of sensitivity to the drug in cells with defects in NER.[11–14] It has in fact been reported that NER-deficient cells are significantly less sensitive to trabectedin than NER-proficient cells. The formation of lethal DNA breaks was reported to be related to a functional transcription-coupled NER pathway (TC-NER).[13,15] Studies in *S.pombe* have suggested that the action of trabectedin in eukaryotic cells might be the result of NER inactivation through the formation of an inactive Rad13/DNA/trabectedin ternary complex, thus conveying the idea that NER components may represent the primary targets of the drug. In the same work, it was shown that trabectedin-induced damage requires DSB repair, suggesting a pivotal role of this pathway in the drug-induced cytotoxicity. Very recent data also suggest that in mammalian cells the homologous recombination repair of DSB is important in modulating the cellular response to trabectedin.[16]

In this paper, we investigated the involvement of these repair pathways in budding yeast and in isogenic mammalian systems, proficient and deficient in DSB repair. Indeed, the data support the conclusion that not only does homologous recombination repair play an important role in the mechanism of the drug action, but also that the formation of trabectedin induced cytotoxic DSBs needs a functional NER pathway.

2. Materials and methods

2.1. *S.cerevisiae strains and colony assay on plate*

The genotype of the yeast strains used in this work is listed in Table 1. The strains are isogenic derivatives of the wild type W303 background, kindly provided by R. Rothstein (Columbia University, NY). The strains were grown in YPD at equal cellular concentration and sequentially diluted 1:6 before being spotted on YPD plates without (UNT) or with the indicated drugs. The drug concentrations used were previously assayed for being sub-lethal for the wt strain. Cellular growth was evaluated after incubation at 28 °C for 3–5 days.

Table 1 – Genotype of the mutant yeast strains studied

Mutant	Stock #	*Genotype*
Wt	W303	*Mata, ade2-1, ura3, trp1-1, leu2-3, leu2-112, his3-15, can1-100, GAL, PSI1+*
mre11	CY2330	W303, *mre11::KanMX4*
RAD51	CY2269	W303, *RAD51::KanMX4*
RAD52	CY2272	W303, *RAD52::KanMX4*
sgs1	CY2570	W303, *sgs1::KanMX4*
top3	CY2284	W303, *top3::KanMX4*
RAD6	CY900	W303, *RAD6::URA3*
RAD18	CY2821	W303, *RAD18::HIS3MX6*
rev3	CY2366	W303, *rev3::KanMX4*
msh2	CY2361	W303, *msh2::KanMX4*
srs2	CY2643	W303, *srs2::KanMX4*
mec1	CY3191	W303, *mec1::KanMX4, sml1::HIS3MX6*
RAD53	CY3205	W303, *RAD53::KanMX4, sml1::HIS3MX6*
tel1	CY2886	W303, srs2::3HA-Srs2, *tel1:: HIS3MX6*
dun1	CY2938	W303, *dun1::KanMX4*
RAD24	CY2054	W303, *RAD24::TRP1*
ku70	SY2149	W303, *ku70::LEU2*
top1	CY2278	W303, *RAD24:: KanMX4*

2.2. *Mammalian cells and culture conditions*

Chinese hamster ovary (CHO) cell lines (AA8, UV-96, V3-3, irs1SF, CXR3, V79, VC8, VC8-BAC, VC8#13-10) were grown in monolayer in Ham's F-10 medium (Cambrex, Bio Science, Verviers, Belgium) containing 10% foetal bovine serum (FBS) (Sigma-Aldrich Co. Ltd, UK), 1% (v/v) L-glutamine (200 mM), 1% (v/v) Hepes (1 M) and 1.6% (v/v) NaHCO3 (7.5%) (Cambrex). XPA human cells were maintained in RPMI-1640 (Cambrex) containing 10% FBS and 1% (v/v) L-glutamine (200 mM). V3-3, irs1SF, CXR3 were kindly provided by Dr. T. Helleday, while V79, VC8, VC8-BAC, VC8#13-10 cells lines were obtained from Dr. M. Zdzienicka. XPA cell line was kindly provided by Dr. Jim Ford (Stanford University School of Medicine, CA, USA) and the complemented cell line was obtained after transfection with human XPA cDNA, kindly provided by Dr. Jim Ford. Stably transfected cells were maintained in medium containing G418 500 μg/ml.

2.3. *Drugs*

Trabectedin, kindly supplied by PharmaMar (Colmenar Viejo, Madrid, Spain), was stocked in DMSO at a concentration of 1 mM; DNA-PKcs inhibitor NU7026 was purchased by Calbiochem (La Jolla, CA, USA) and stocked in DMSO at 10 mM, cis-DDP was purchased from Sigma-Aldrich (St. Louis, MO, USA). All the drugs were diluted in warm medium just before use.

2.4. *Cytotoxicity assays*

For clonogenic assays, cells were plated at 150 cell/ml and after 48 h were treated for 1h with different drug concentrations. Colonies were stained with 1% crystal violet (Sigma-Aldrich) after 7–10 days and counted using the Entry Level Image analysis system (Immagini & Computer, Bareggio, Milan, Italy). In growth inhibition assays, exponential growing cells were treated for 24 h with different concentrations of trabectedin, pre-incubated or not, for 1h with 20 μM DNA-PKcs inhibitor. Cells were counted 72 h after drug removal.

2.5. *Flow cytometric γ-H2AX detection*

γ-H2AX was detected by a flow cytometric assay. Briefly, cells were fixed in 1% formaldehyde-methanol free and in 70% ethanol; then permeabilised with 0.5% saponin and incubated for 1 h with anti-phospho-histone H2AX (1:20000). After washing with 1% saponin, the secondary antibody (goat anti-mouse Alexa-Fluor 488, Molecular Probes, Leiden, The Netherlands, 1:800) was added for 1 h. DNA was stained with 1 ml of a solution containing 0.5 μM TO-PRO-3 iodide (TP3) and 25 μl RNAse 1% in PBS. Flow cytometric analysis was performed on at least 20,000 cells by using FACS Calibur instrument. To calculate the mean fluorescence intensity of γ-H2AX antibody staining in arbitrary units, background signal was subtracted. The data

represent the average of three replicates and were analysed using Cell Quest software.

2.6. Immunocytochemical γ-H2AX and Rad51 foci detection

At different times after drug wash-out, cells, grown on glass cover slips, were washed with PBS and processed for γ-H2AX staining as described for the cytometric detection, except for TP3, substituted by Hoechst 33358. Rad51 foci were detected as already described,[17] with minor modification. For both detections, slides were mounted with FluorSave Reagent (Calbiochem) and analysed using an Olympus BX60 fluorescence microscope with a 100X UPIanAPO objective. For Rad51 foci quantitation, 200 cells/point were counted.

3. Results

3.1. DSB repair is required to survive to trabectedin treatment in S.cerevisiae

We evaluated the sensitivity to trabectedin of mutants in genes required for DSB repair (*MRE11*, *RAD51*, *RAD52*, *KU70*), replication fork restart (*SGS1*, *TOP3*), post-replicative repair (PRR) (*RAD6*, *RAD18*, *REV3*, *SRS2*), mismatch repair (*MSH2*), DNA topology (*TOP1*) and DNA damage checkpoint activation (*MEC1*, *TEL1*, *DUN1*, *RAD24*). We used a drug concentration that is sub-lethal in wt cells (data not shown). At this concentration, only mutants in the homologous recombination pathway -*mre11, rad51 and rad52* (Fig. 1) exhibited hypersensitivity to trabectedin. *ku70* and *dun1* mutants also showed a mild sensitivity. We also treated the same mutants with Methylmethane sulphonate (MMS) and Cisplatin (DDP), the former is a methylating agent and the latter causes intra- and interstrand cross-links. Both treatments interfere with the replicative fork progression resulting in the formation of DNA breaks during replication. As shown in Fig. 1, MMS and DDP treatments require the PRR and DSB repair pathways for survival. Hence, the cytotoxic profile of trabectedin differs from the ones of MMS and DDP relatively to the requirement of post replicative repair genes.

3.2. Effect of trabectedin on mammalian systems deficient and proficient in DNA-DSB repair

The increased sensitivity of trabectedin in yeast mutants lacking a functional DSB repair prompted us to investigate its cytotoxic activity in a number of mammalian systems deficient and proficient in repairing DSBs. These lesions are repaired in mammalian cells by two distinct mechanisms: the non-homologous end-joining (NHEJ) and the recombinational repair (HR) (for review see[18,19]). The NHEJ pathway is considered error-prone as the two exposed DNA termini are simply processed and ligated together; on the contrary, HR requires the presence of an identical or near identical sequence and is error free. We have already reported a 2–3-fold increased

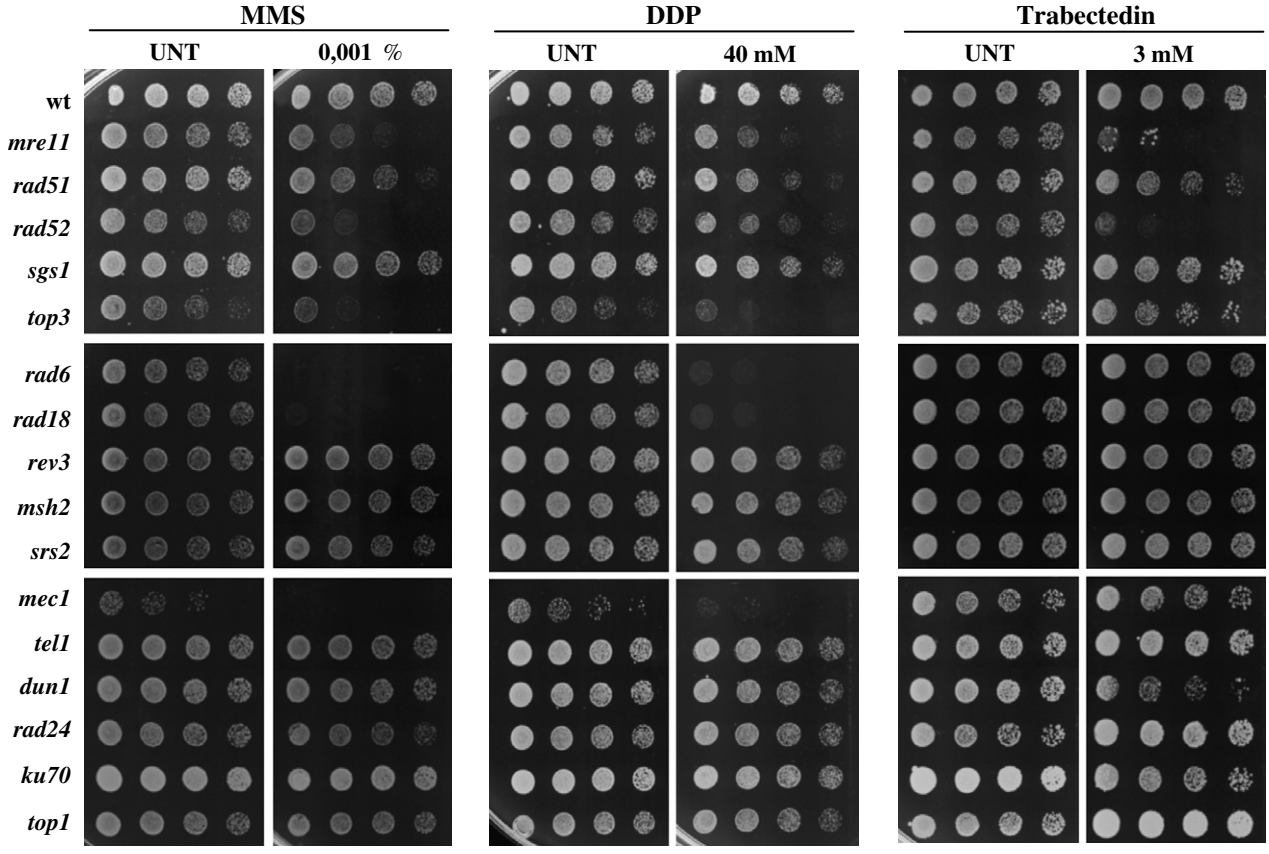

Fig. 1 – Cytotoxic activity of MMS, cisplatin and trabectedin in isogenic yeast mutants. The mutant genotype is listed in Table 1.

sensitivity in human glioblastoma cell with a mutation in the catalytic domain of DNA-PK (M059J) compared to wild type cells (M059K).[11] However the system is not syngenic, as two paired cell lines were obtained from different fragments of the tumour biopsy and thus they could carry more differences that the one found on DNA-PKcs.[20] To better investigate the role of NHEJ, we selected a CHO derived cell line lacking DNA-PK (V3-3 cell line) and its wt counterpart (AA8). As shown in Fig. 2 (panel A), a partial sensitisation could be observed with V3-3 cells being 2-fold more sensitive to trabectedin treatment (IC50s 8.2 ± 1.9 versus 15.2 ± 3.25). These data are corroborated by experiments in which the co-treatment with NU-7026, a specific inhibitor of DNA-PKcs, causes a partial sensitisation in AA8 cells (Fig. 2, panel B).

We then tested rodent cell lines with deficiencies in HR repair due to specific functional inactivation in *XRCC3* gene (irs1SF cell line), a Rad51 paralog, and in *XRCC11* gene, (VC8 cell line), a BRCA2 paralog and in cell lines derived from them, in which the defect has been complemented by transfection with the corresponding lacking gene. The products of the above genes (XRCC3 and XRCC11) have a key role in HR.[21,22] As depicted in Fig. 2, panel C, a 10-fold increase in trabectedin sensitivity was observed in irs1SF cells, lacking a functional XRCC3, while the pattern of sensitivity reversed in irs1SF cells transfected with the *XRCC3* gene (CXR3 cell line). A more dramatic increase in trabectedin sensitivity was observed (approximately a 100-fold) in cells with BRCA deficiency (Fig. 2, panel D), with an almost complete reversal of the drug activity in VC8 complemented cells VC8-BAC and VC8#13-10, These data strongly suggest that HR pathway is also involved in the processing of trabectedin-induced DNA lesions in mammalian cells.

3.3. *Rad51 foci formation by trabectedin treatment in CHO NER proficient and deficient cells*

We then reasoned that if HR is important for trabectedin cytotoxicity, the drug treatment should induce the formation of Rad51 foci, considered foci where DNA DSBs are processed.[23,24] We investigated the kinetics of Rad51 foci formation after trabectedin treatment in AA8 cell lines and in its subline UV-96, NER deficient due to a functional inactivation of ERCC1. We chose this cellular system as it was previously characterised for a different sensitivity to trabectedin cytotoxic activity being NER efficient cells less sensitive to the drug (Fig. 3, panel A). Untreated UV-96 cells did display a

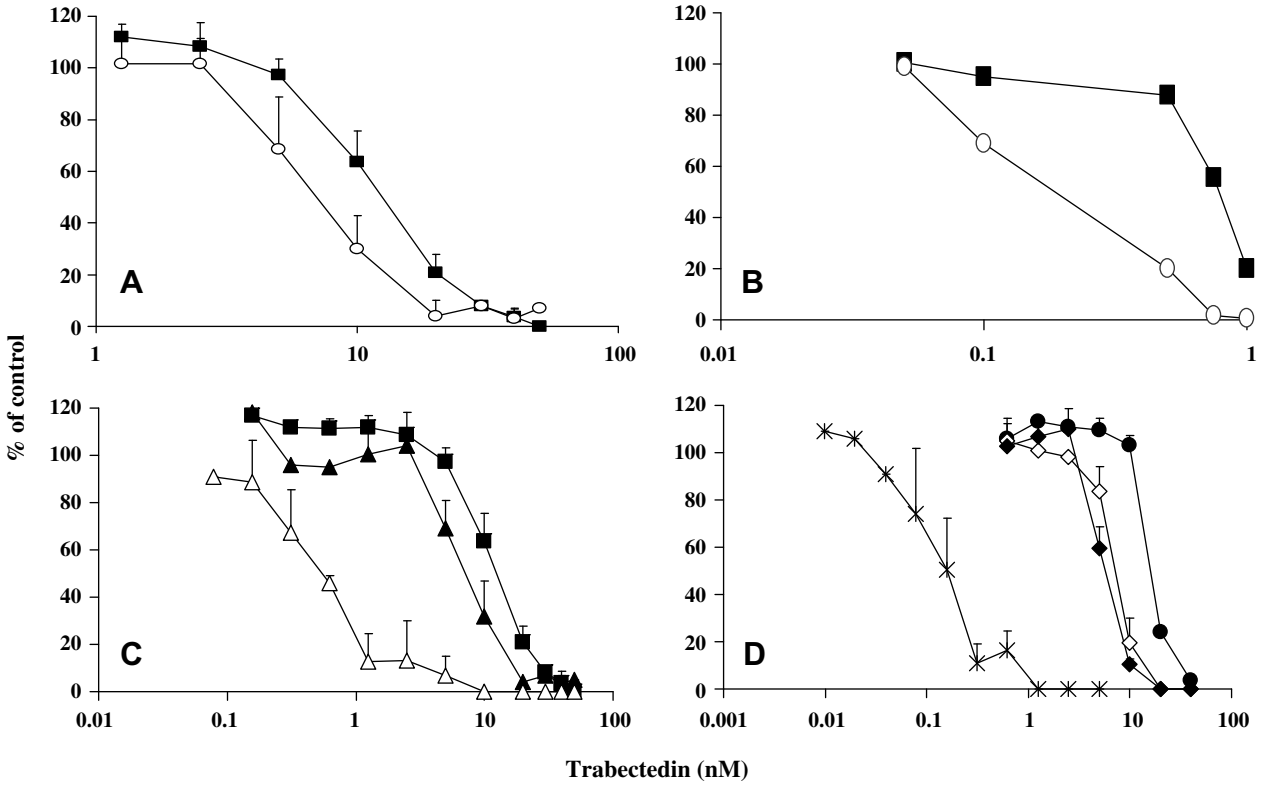

Fig. 2 – Effect of 1 h trabectedin exposure on the clonogenicity of CHO cell lines (panels A, C and D). Each point is the mean ± SD of three experiments, each run in five replicates. Panel A. AA8: wild type cell line (■); V3-3: DNA-PKcs deficient cell line (○). Panel C. AA8 cell line (■); irs1SF : XRCC3 deficient cell line (△); CXR3 cell line: irs1SF XRCC3 cell line complemented with human *XRCC3* (▲). Panel D. V79: wild type cell line (●); VC8 cell line: BRCA2 deficient cell line (×); VC8-BAC cell line: VC8 cell line complemented with human BRCA (◇); VC8#13-10 cell line: VC8 cell line complemented with the entire human chromosome 13 containing BRCA2 (♦). Panel B. Growth inhibition induced on AA8 cell line by 24 h exposure to trabectedin alone (■) or after 1 h pre-incubation with 20 μM DNA-PKcs inhibitor, NU7026 (○). Each point is the mean ± SD of three experiments each run in triplicates.

2-fold increase in the % of cells positive for Rad51 foci (33 ± 3 versus 15 ± 2 in AA8 cells). This is probably due to the fact that UV-96 cells are NER deficient and can cope less efficiently with endogenous damage. At the trabectedin concentration of 20 nM, corresponding in AA8 to the IC_{50}, the number of Rad51 foci increased with time reaching a peak at 4 h and started to decline 48 h after drug washout (panel B). On the contrary, on UV-96 cells, no increase in the % of cells positive for Rad51 foci was observed at the same concentration, corresponding to an IC_{10}, while a slight increment was observed at the higher dose of 80 nM, corresponding to an IC_{50}, starting from 8 h and peaking at 24 h after drug washout. The increase in Rad51 foci did not, however, reach the magnitude found in AA8. Differently from AA8 cells, Rad51 foci almost completely disappeared by 48 h in UV-96, suggesting that trabectedin induces Rad51 foci formation only in the presence of an active NER process.

3.4. γ-H2AX phosphorylation induced by trabectedin treatment in NER proficient and deficient cells

H2AX is a histone H2A variant that is specifically phosphorylated at Ser139 upon DSB induction and has been widely used as a marker for the presence of DSBs.[25,26] We assayed the kinetics of γ-H2AX induction by flow cytometry after trabectedin treatment both in AA8 and UV-96 cells.

The biparametric γ-H2AX/DNA content analysis of untreated and treated AA8 and UV-96 cells are shown in Fig. 4. As already reported for Rad51 foci, a higher % of cells positive for γ-H2AX was observed in control UV-96 cells than in control AA8 cells. Based on differences in DNA content, it was possible to discriminate between G_1, S and G_2M cell population and correlate the drug-induced increase in phosphorylation of H2AX to the cell cycle phases.

In AA8 cells (Fig. 4, Panel A, left), already at 1 h after drug-washout, γ-H2AX increased mainly from S-early to G_2M phase in treated cells. At 24 h, the percentage of S-G_2M blocked γ-H2AX positive cells strongly increased in a dose dependent manner, (panel A). At 20 nM, trabectedin induced a complete S-G_2M block. The fraction of positive γ-H2AX treated cells was 4.5 and 5-fold compared with the control ones for 5 and 20 nM trabectedin respectively (data not shown). Considering the mean intensity, the maximum level of γ-H2AX mean fluorescence was reached already at 1 h after drug-washout in S phase cells. At 24 h there was a decrease of γH2AX in S phase cells, while an increase was detected in G_2M and G_1 phases in cells treated with the higher concentration (Panel B, left).

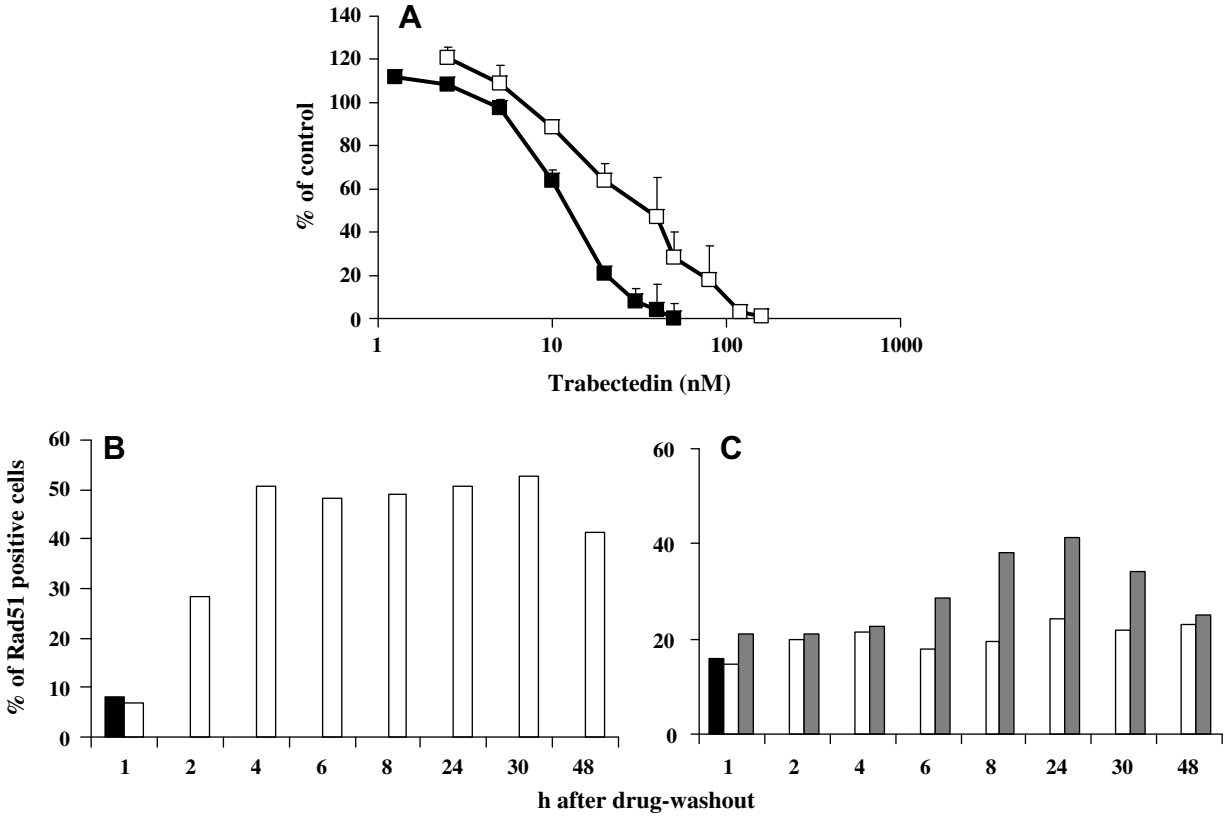

Fig. 3 – Panel A. Effect of 1 h trabectedin exposure on the clonogenicity of CHO cell lines. Each point is the mean ± SD of three experiments, each run in five replicates. AA8 cell line (■); UV-96 cell line, NER deficient due to a non functional ERCC1 gene (□). Panel B. Percentage of Rad51 positive AA8 cells at different time intervals after drug-washout. Control (■); trabectedin 20 nM (□). Panel C. Percentage of Rad51 positive UV-96 cells at different time intervals after drug-washout. Control (■); trabectedin 20 nM (□); trabectedin 80 nM (▩).

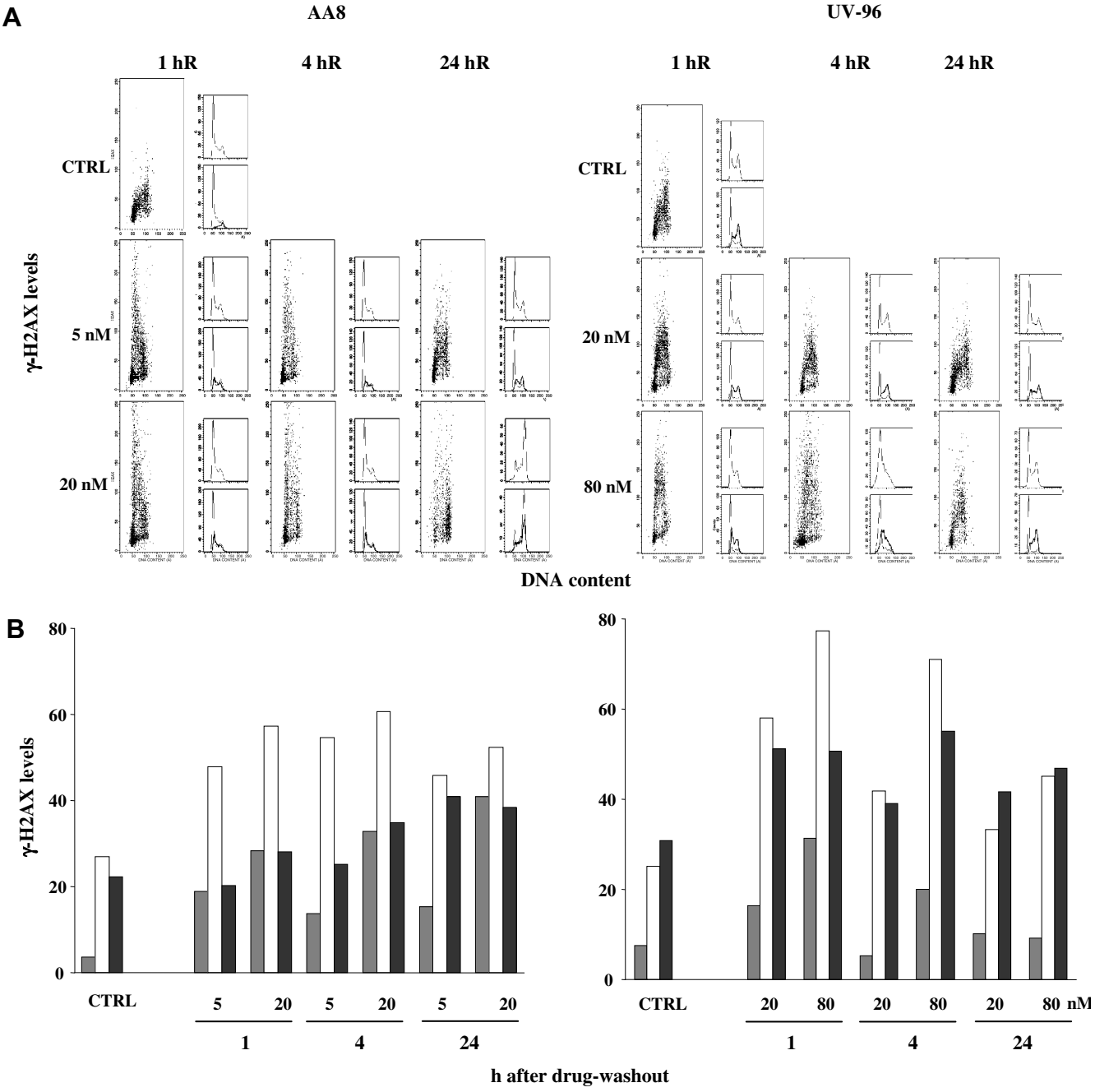

Fig. 4 – Panel A. Flow cytometric analysis of γ-H2AX levels in AA8 (left side) and UV-96 cell lines (right side) evaluated at different time points after trabectedin treatment. Total DNA content is shown in the upper histograms, while in the lower histograms are represented the DNA content of γ-H2AX-negative cells (thin line) and of γ-H2AX-positive cells (bold line). Panel B. Mean γ-H2AX intensity levels related to the different cell cycle phase distribution in both AA8 and UV-96 cell lines evaluated at 1, 4 and 24 h after drug-washout. ■: G_1, □: S, ■: G_2M.

In UV-96 cells treated with the drug (Fig. 4, right), the increase in γ-H2AX was less marked and less prominent than in AA8 cells. At 1 h after drug-washout the γ-H2AX positive cells were distributed from S-early to G_2M phase and the fraction of S-early cells increased at 80 nM. 4 h after drug-washout the majority of γ-H2AX positive cells were in S and G_2M phases in cells treated with 20 nM and in S phase at a drug concentration of 80 nM. At 24 h after drug-washout, the γ-H2AX positive cells were in S-G_2M phases while the negative were mostly in G_1. No significant G_2M block was observed in UV-96 cells after trabectedin treatment, as already reported.[27] The fraction of positive γ-H2AX trabectedin treated cells was 1.3-fold compared to control ones for both concentrations, with an almost complete recovery by 24 h. The quantitative analysis of mean γ-H2AX intensity showed that the maximum level of γ-H2AX mean fluorescence was reached already at 1 h after drug-washout in S phase cells, as for AA8 cells. At 24 h after drug-washout, the level of γ-H2AX decreased and

was similar at both drug concentrations (Panel B, right). These data were corroborated by immunofluorescence analysis (Supplementary information, Fig. 1).

The fact that γ-H2AX could be detected after trabectedin treatment mainly in a NER proficient cellular system suggests that the DSBs are not directly caused by the drug, but are formed during the processing/repair of the lesions. In addition, the maximum level of γ-H2AX detected in cells of the S phase at an early time point (1 h recovery) suggests that during DNA synthesis the drug-induced lesion is converted to DNA-DSB. Previous data from our laboratory in different cellular systems clearly showed that no DNA double strand breaks could be detected by alkaline elution and comet assay at different concentrations and time intervals after trabectedin treatment .[10] These contrasting results could be explained by the higher resolution of the γ-H2AX detection technique.

3.5. *Rad51 foci formation and H2AX phosphorylation induced by trabectedin treatment in human cells deficient and proficient in NER*

To corroborate these findings, we performed similar experiments using a human cellular system. Immortalised human XPA–/– fibroblasts were stably transfected with human XPA cDNA to obtain a complemented XPA-cell line. As depicted in Fig. 5, panel A cells complemented with XPA were more sensitive to the cytotoxic effects of trabectedin. The cell cycle perturbation in both XPA –/– and XPA+/+ clearly indicated a dose-dependent G_2M block in XPA+/+ cells (sensitive to the drug), while a slight G_2M block could be observed in XPA–/– cells at the highest drug dose tested at 24 h (Fig. 5, panel B). We then analysed the Rad51 foci formation and the induction of γ-H2AX after drug treatment (Fig. 5, panel C and D). Trabectedin induced an increase in Rad51 foci at both the doses tested that peaked at 4 h after the end of treatment and persisted up to 24 h in XPA complemented cells; on the contrary, only a modest increment could be observed in XPA–/– cells with the highest dose (30 nM) at 24 h. Similarly, a higher increase in γ-H2AX positive cells, in particular cells in the S and G_2-M phases of the cell cycle, could be detected in XPA complemented cells at both doses starting from 4 h after drug removal. In XPA–/– cells, a slight increase in γ-H2AX stained cells was observed with the highest dose at 24 h. The Rad51 foci formation and the induction of γ-H2AX in this system mirrored what has been described in the CHO NER proficient /deficient system.

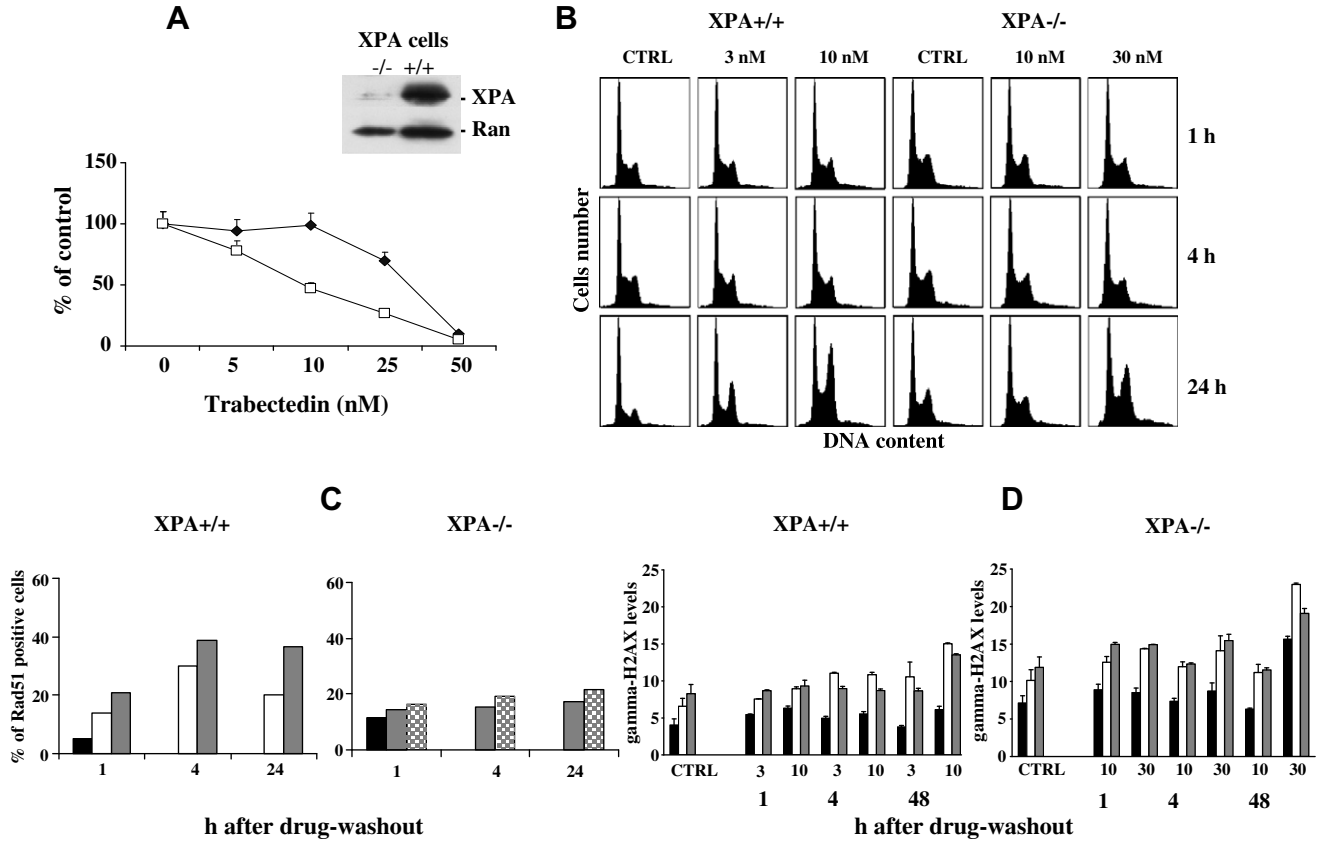

Fig. 5 – Panel A. Dose response curve in XPA–/–, NER deficient cell line (◆) and XPA +/+ cells, complemented with human XPA (□) after 1 h treatment with trabectedin. Panel B. Cell cycle perturbations induced by 1 h exposure with trabectedin in XPA+/+ (3 or 10 nM) and XPA–/– (10 or 30 nM) cell lines evaluated at different times intervals after drug-washout. Panel C. Percentage of Rad51 positive XPA+/+ (left) and XPA–/– (right) cells. Control (■); trabectedin 3 nM (□); trabectedin 10 nM (▩); trabectedin 30 nM (▨)). Panel D. Mean γ-H2AX intensity levels related to the different cell cycle phase distribution in XPA+/+ and XPA–/– cell lines evaluated at different time intervals after drug-washout. G_1(■); S (□); G_2M (▩).

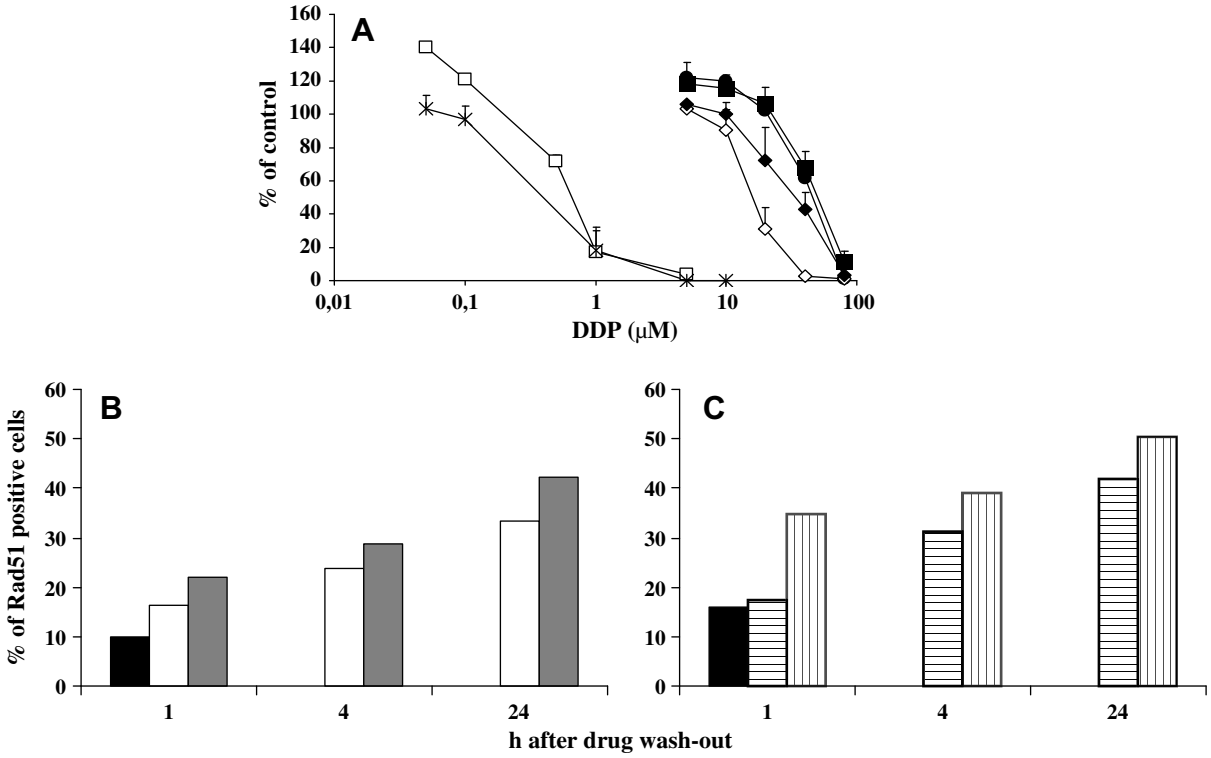

Fig. 6 – Panel A. Effect of 1 h DDP treatment on the clonogenicity of CHO cell lines. Each point is the mean of three experiments ± SD, each run in five replicates. AA8 (■); UV-96 (□); V79 (●); VC8 (∗); VC8-BAC (◇); VC8#13-10: (◆). Panel B: Percentage of Rad51 positive AA8 cells evaluated at different time intervals after DDP washout. Control (■); DDP 30 μM, (□) ; DDP 60 μM (▤). Panel C: Percentage of Rad51 positive UV-96 cells evaluated at different time intervals after DDP washout. Control (■); DDP 0.5 μM (▤); DDP 1 μM (▥).

3.6. *Rad51 foci formation induced by Cis-platinum (DDP) treatment in CHO cells deficient and proficient in NER*

We finally analysed the effect of DDP treatment in CHO NER proficient and deficient cells. UV-96 cells are extremely sensitive to DDP, with a 100-fold increase in sensitivity over AA8 cells (Fig. 6, panel A). The observed increased sensitivity is similar to the one observed in cell lacking a functional recombinational repair (Fig. 6, panel A). The extreme sensitivity to DDP in cell lacking ERCC1 and HR has already been reported and has been associated with the inability to repair the interstrand cross-links induced by DDP. When the kinetics of Rad51 foci formation were studied after DDP treatment, a similar induction (both in magnitude and in a temporal fashion) was observed starting from 1 h after drug washout and persisting up to 24 h in both NER proficient and deficient cells. These results suggest that Rad51 foci formation is not dependent, as in the case of trabectedin-induced lesions, on a functional NER, but on the contrary, the DDP-induced lesions are recognised in both NER proficient and deficient cells.

4. Discussion

Trabectedin has been shown to bind to N2 guanine in the minor groove of DNA,[8] and this interaction is such that it causes a structural bending of DNA towards the minor groove, causing an unusual DNA helix distortion.[28] This lesion is a substrate for the NER pathway. In fact, yeast, hamster cells and human cells deficient in NER are resistant to trabectedin, with fold resistance ratios ranging from 2 to 10.[12,29,30] This is unusual, intriguing and somewhat paradoxical as deficiency in NER is generally associated to an increased sensitivity to DNA interacting agents.[29] It was reported that the NER function was related to the ability of the TC-NER subpathway to induce lethal single strand breaks.[12] Even if recently DSB could be detected by comet assay in HeLa cells after cytotoxic trabectedin doses,[16] several other studies showed no DNA breaks, assessed both by alkaline elution and by the comet assay after trabectedin treatment, unless with drug concentrations 100 times higher than the IC_{50}.[10,14] These contrasting results might be due to the different systems used and still render controversial the ability of trabectedin in inducing a quantifiable number of DNA breaks.

Recent data support the role of HR in the drug induced cytotoxicity. Mammalian HR-deficient cells displayed hypersensitivity to the drug[16] and, in addition, data produced in the fission yeast *S. pombe* suggested a crosstalk between the NER and HR pathways to deal with trabectedin-induced lesions.[15] In the proposed model, the trabectedin adducts in the minor groove are recognised by the NER system, in particular the XPG protein. The catalytic endonuclease activity of the Rad13 (yeast homolog of XPG) protein was found to be dispensable, while its C terminal region was essential for the formation of 'cytotoxic complexes' that during the S phase give

rise to lesions, probably DSBs, that need to be repaired by HR. Both studies suggested that the trabectedin induced DNA adducts are likely to be converted to cytotoxic DSBs in S phase.

In the present study we screened *S.cerevisiae* mutants defective in the main DNA repair pathways. This assay revealed that DSB repair mutants are specifically sensitive to trabectedin, indicating that HR pathway is mainly required to face the effects of the treatment, while NHEJ mutants are only mildly more sensitive to the drug. The evidence that HR mutants are very sensitive to trabectedin is in keeping with the previous findings in *S.pombe*. The requirement of Dun1 checkpoint kinase to deal with trabectedin could similarly reflect the function of Dun1 in modulating DSBs repair. Surprisingly, PRR mutants did not show hypersensitivity to trabectedin, while they are usually sensitive to other S-phase damaging agents (Fig. 1). In yeast and human cells, both HR and NHEJ pathways are involved in DSB repair, with HR acting mainly in G_2-M phase and NHEJ in G_1 phase of the cell cycle. Since in *S.cerevisiae*, NHEJ is also required after trabectedin treatment, we decided to investigate the roles of the two DSB repair pathways in isogenic mammalian cells. Cells deficient in NHEJ were approximately 2-fold more sensitive to trabectedin than proficient cells, as already reported.[11] Similar increase in sensitivity was observed treating wild type cells with a specific DNA-PKcs inhibitor, suggesting a limited role of NHEJ pathway in processing trabectedin-induced DNA lesions. Cells lacking HR pathway were indeed extremely sensitive to the drug with a decrease in IC_{50} of about 100-fold. Complementation of the defects almost completely reverted the sensitivity to normal control level, strongly suggesting that HR is a key determinant in repairing trabectedin-induced lesions. Considering that NER deficiency confers resistance to the drug, that HR is determinant for the processing of the DNA lesions, that HR generally processes DNA-DSBs, we attempted to explore this cross-connection studying the involvement of HR in pairs of cell lines proficient and deficient of NER, by monitoring the activation of γ-H2AX and Rad51 foci formation. Trabectedin treatment induced both γ-H2AX and Rad51 foci formation in NER proficient cells, suggesting the formation of DSBs in DNA that are tentatively repaired by the induction of Rad51 foci. On the other hand, both events were clearly much less evident in a NER deficient background, suggesting that in the presence of trabectedin, the NER pathway is responsible for the incision/excision of the DNA lesion leading to the formation of DSBs. In addition, the induction of γ-H2AX is much more evident in the S phase of the cell cycle, corroborating the hypothesis put forward by Soares et al.[16] of a strict requirement for DNA synthesis in the formation of trabectedin induced DSBs. The fact that only in NER proficient cells a clear-cut induction of H2AX phopshorylation and Rad51 foci formation was observed can be explained in the light of what was found in *S.pombe*, where the formation and stabilisation of a ternary complex among DNA trabectedin and the Rad13 carboxy-terminal region was responsible for the drug cytotoxicity. This suggests that the NER proficiency leads to the accumulation of unprocessed SSBs that can be converted to DSB in S phase. In AA8 and UV-96 cells, respectively NER proficient and NER deficient, DDP treatment was able to induce the formation of Rad51 foci in both cells regardless of the cell NER status, suggesting that the extreme sensitivity of UV-96 cells to DDP is probably due to the repair inability of the cells and not to factors involved in the initial recognition of the lesions. In contrast, in the case of trabectedin, the inability of NER deficient cells to efficiently activate the induction of Rad51 foci appears to have a protective role.

The unravelling of the molecular mechanism of the DNA repair pathways and the cumulating evidence of the existence of a sub-set of tumours with specific defect in the HR DNA repair pathway, the so called BRCAness phenotype,[31–34] clearly suggest that patients whose tumours harbour those specific defects should better benefit from a trabectedin based therapy. This concept will have to be tested in the clinic.

Conflict of interest statement

None declared.

Acknowledgement

M.T. is a recipient of the "Vittorio Ferrari" FIRC fellowship. I.C. was funded by AIRC Unicredito Italiano fellowship and by UICC/ICRETT fellowship. The generous contribution of the Italian Association for Cancer Research (AIRC) and the Nerina and Mario Mattioli Foundation are greatly acknowledged.

REFERENCES

1. D'Incalci M, Colombo T, Ubezio P, et al. The combination of yondelis and cisplatin is synergistic against human tumor xenografts. *Eur J Cancer* 2003;**39**(13):1920–6.
2. D'Incalci M, Erba E, Damia G, et al. Unique features of the mode of action of ET-743. *Oncologist* 2002;**7**:210–6.
3. Le Cesne A, Blay JY, Judson I, et al. Phase II study of ET-743 in advanced soft tissue sarcomas: A European Organisation for the Research and Treatment of Cancer (EORTC) Soft Tissue and Bone Sarcoma Group Trial. *J Clin Oncol* 2005;**23**(3):576–84.
4. Sessa C, de Braud F, Perotti A, et al. Trabectedin (ET-743) for women with ovarian carcinoma after treatment with platinum and taxanes fails. *J. Clin. Oncol.* 2005;**23**:1867–74.
5. Fayette J, Coquard IR, Alberti L, et al. ET-743: a novel agent with activity in soft-tissue sarcomas. *Curr Opin Oncol* 2006;**18**(4):347–53.
6. Grosso F, Forni C, Frapolli R, et al. Sensitivity of myxoid-round cell liposarcoma (MRCL) to trabectedin (T) may be related to a direct effect on the fusion transcript. J Clin Oncol, 2007 ASCO Annual Meeting Proceedings Part I 2007;25 (June 20 Suppl.)(18S):10000.
7. Grosso F, Jones RL, Demetri GD, et al. Efficacy of trabectedin (ecteinascidin-743) in advanced pretreated myxoid liposarcomas: a retrospective study. *Lancet Oncol* 2007;**8**:595–602.
8. Pommier Y, Kohlhagen G, Bailly C, Waring M, Mazumder A, Kohn KW. DNA sequence- and structure-selective alkylation of guanine N2 in the DNA minor groove by ecteinascidin 743, a potent antitumor compound from the caribbean tunicate Ecteinascidia turbinata. *Biochemistry* 1996;**35**:13303–9.
9. Moore II BM, Seaman FC, Hurley LH. NMR-based model of an ecteinascidin 743-DNA adduct. *J.Am.Chem.Soc.* 1997;**119**:5475–6.

10. Erba E, Cavallaro E, Damia G, et al. The unique biological features of the marine product Yondelis™ (ET-743, trabectedin) are shared by its analog PM00128 which lacks the C ring. *Oncol Res* 2004;**14**(11-12):579–87.
11. Damia G, Silvestri S, Carrassa L, et al. Unique pattern of ET-743 activity in different cellular systems with defined deficiencies in DNA-repair pathways. *Int J Cancer* 2001;**92**(4):583–8.
12. Takebayashi Y, Pourquier P, Zimonjic DB, et al. Antiproliferative activity of ecteinascidin 743 is dependent upon transcription-coupled nucleotide-excision repair. *Nat Med* 2001;**7**(8):961–6.
13. Soares DG, Poletto NP, Bonatto D, Salvador M, Schwartsmann JA, Henriques JA. Low cytotoxicity of ecteinascidin 743 in yeast lacking the major endonucleolytic enzymes of base and nucleotide excision repair pathways. *Biochem Pharmacol* 2005;**70**(1):59–69.
14. Erba E, Bergamaschi D, Bassano L, et al. Ecteinascidin-743 (ET-743), a natural marine compound, with a unique mechanism of action. *Eur J Cancer* 2001;**37**(1):97–105.
15. Herrero AB, Martin-Castellanos C, Marco E, Gago F, Moreno S. Cross-talk between nucleotide excision and homologous recombination DNA repair pathways in the mechanism of action of antitumor trabectedin. *Cancer Res* 2006;**66**(16):8155–62.
16. Soares DG, Escargueil AE, Poindessous V, et al. Replication and homologous recombination repair regulate DNA double-strand break formation by the antitumor alkylator ecteinascidin 743. *Proc Natl Acad Sci U S A* 2007;**104**(32):13062–7.
17. Bashkirov VI, King JS, Bashkirova EV, Schmuckli-Maurer J, Heyer WD. DNA repair protein Rad55 is a terminal substrate of the DNA damage checkpoints. *Mol Cell Biol* 2000;**20**(12):4393–404.
18. Sekiguchi JM, Ferguson DO. DNA double-strand break repair: a relentless hunt uncovers new prey. *Cell* 2006;**124**(2):260–2.
19. Wyman C, Kanaar R. DNA double-strand break repair: all's well that ends well. *Annu Rev Genet* 2006;**40**:363–83.
20. Lees-Miller SP, Godbout R, Chan DW, et al. Absence of p350 subunit of DNA-activated protein kinase from a radiosensitive human cell line. *Science* 1995;**267**(5201):1183–5.
21. Sonoda E, Zhao GY, Kohzaki M, et al. Collaborative roles of gammaH2AX and the Rad51 paralog Xrcc3 in homologous recombinational repair. *DNA Repair (Amst)* 2007;**6**(3):280–92.
22. Wiegant WW, Overmeer RM, Godthelp BC, van Buul PP, Zdzienicka MZ. Chinese hamster cell mutant, V-C8, a model for analysis of Brca2 function. *Mutat Res* 2006;**600**(1-2):79–88.
23. Mladenov E, Anachkova B, Tsaneva I. Sub-nuclear localization of Rad51 in response to DNA damage. *Genes Cells* 2006;**11**(5):513–24.
24. Yonetani Y, Hochegger H, Sonoda E, et al. Differential and collaborative actions of Rad51 paralog proteins in cellular response to DNA damage. *Nucleic Acids Res* 2005;**33**(14):4544–52.
25. Foster ER, Downs JA. Histone H2A phosphorylation in DNA double-strand break repair. *Febs J* 2005;**272**(13):3231–40.
26. Lowndes NF, Toh GW. DNA repair: the importance of phosphorylating histone H2AX. *Curr Biol* 2005;**15**(3):R99–R102.
27. Tavecchio M, Natoli C, Ubezio P, Erba E, D'Incalci M. Dynamics of cell cycle phase perturbations by Trabectedin (ET-743) in NER deficient and proficient cells, unravelled by a novel mathematical simulation. *Cell Prolif* 2007;**40**(6):885–904.
28. Zewail-Foote M, Hurley LH. Ecteinascidin 743: a minor groove alkylator that bends DNA toward the major groove. *J.Med.Chem.* 1999;**42**:2493–7.
29. Damia G, Imperatori L, Stefanini M, D'Incalci M. Sensitivity of CHO mutant cell lines with specific defects in nucleotide excision repair to different anti-cancer agents. *Int J Cancer* 1996;**66**(6):779–83.
30. Zewail-Foote M, Li VS, Kohn H, Bearss D, Guzman M, Hurley LH. The inefficiency of incisions of ecteinascidin 743-DNA adducts by the UvrABC nuclease and the unique structural feature of the DNA adducts can be used to explain the repair-dependent toxicities of this antitumor agent. *Chem Biol* 2001;**8**(11):1033–49.
31. Kennedy RD, D'Andrea AD. DNA repair pathways in clinical practice: lessons from pediatric cancer susceptibility syndromes. *J Clin Oncol* 2006;**24**(23):3799–808.
32. Turner N, Tutt A, Ashworth A. Hallmarks of 'BRCAness' in sporadic cancers. *Nat Rev Cancer* 2004;**4**(10):814–9.
33. Lord CJ, Garrett MD, Ashworth A. Targeting the double-strand DNA break repair pathway as a therapeutic strategy. *Clin Cancer Res* 2006;**12**(15):4463–8.
34. Damia G, D'Incalci M. Targeting DNA repair as a promising approach in cancer therapy. *Eur J Cancer* 2007;**43**(12):1791–801.